15. Post-impact Erosion and Sedimentation ❖❖❖

Although the crater is often described as the best preserved impact site on Earth, it has, nonetheless, been weathered, eroded, and modified by secondary sedimentary deposits. Our attention is usually riveted by the geologic processes associated with impact cratering, but it is necessary to also understand how post-impact processes modified the surviving evidence. Also, those secondary processes are, themselves, interesting and a few of them can be used as proxies for crater modification elsewhere in the Solar System, such as Mars.

I begin with some of the most commonly observed features seen on the crater rim. I also begin with the processes that affect Kaibab ejecta, because that is the material that dominates the crater rim and ejecta blanket. As already noted in Chapter 2, the surface of Kaibab is often textured with dissolution pits (Fig. 15.1). One can find near-vertical alignment of solution pits reflecting water flow downward along the face of boulders. In some cases, the orientations of those features indicate the boulders have shifted or rolled. Dissolution also accentuates fractures in Kaibab and can, in extreme cases, reduce a large boulder to several smaller boulders that fit together like puzzle pieces, separated only by fissures opened by that dissolution (Fig. 15.2).

The dissolution pits in Kaibab are also sometimes called tafoni. In a study of pits in rock at the crater, Norwick and Dexter (2002) used the term tafoni for pits of all sizes, ranging from small, centimeter-scale dissolution pits to larger, meter-scale cavernous openings in the crater wall. Cavernous features occur in both the Kaibab and Moenkopi (Norwick and Dexter, 2002; Kring and Andes, 2015). Examples of tafoni at all scales are shown in Fig. 15.3 and 15.4. The depth of tafoni is a potential geochronometer of rock surface ages throughout the American Southwest. Because Barringer Meteorite Crater has a relatively well-known age, it was used to calibrate that geochronometer. For more details, I refer readers to Norwick and Dexter (2002). In contrast to the nomenclature of Norwick and Dexter (2002), other investigators will reserve the term tafoni for only the largest (m-scale) pits, using instead the term alveoli for cm-scale features. I might add that a new study of cavernous weathering and other rock breakdown features in the Moenkopi and Coconino is underway by a student, Ankit Verma, and his advisor, Mary Bourke, so interested readers should look for those results in the near future.

Caliche is commonly associated with Kaibab pebbles, cobbles, and boulders along the rim and in the ejecta blanket. These bright white coatings are produced when calcium, dissolved from surface-exposed rocks, re-precipitates in the soil (Fig. 15.5). Exposed caliche around the base of boulders indicate up to 12 inches of erosion has occurred along the rim trail due to people passing. Microscopically, one can see the layers of carbonate are commonly 0.3 to 0.5 mm thick (Fig. 15.6). The coatings may entrain other particles in the soil around a cobble. The coatings may also include phyllosilicates (clay). Multiple layers with variable proportions of carbonate and clay may reflect changing climate. While caliche is most commonly seen around Kaibab, it also coats Moenkopi and Coconino (Fig. 15.5). As noted in Chapter 11, the thickness of these coatings is another potential geochronometer of the crater's age. Based on an observed thickness of 0.5 mm, an age of 54^{+10}_{-8} ka can be calculated. Comparisons of caliche around Barringer Crater samples and caliche around other lithologies (*e.g.*, basalt; Fig. 15.4 and 15.7) in the Flagstaff area exist for those wanting to examine this issue further (Cernok and Kring, 2009; Hörz *et al*., 2016).

Percussion marks is another signature of rock breakdown, but their occurrence is rare as sediment transport is not very energetic and occurs over short distances. Percussion marks are usually found at the base of crater wall cliffs and in the levees of debris flows (see below).

Barringer Meteorite Crater is a closed basin that provides a fascinating opportunity to study erosion caused by variable climate and hydrological conditions. Significant mass wasting is evident along the crater walls, which are cut by dramatic gullies that feed boulder-rich deposits on the crater floor. Two major studies of those processes (Kumar *et al*., 2010; Palucis *et al*., 2012a,b; Palucis *et al.*, 2015) occurred during the past decade and, in both cases, implications for gullies on Mars were explored.

Each gully is composed of an alcove, a channel, and a depositional zone. The alcoves are excavated from bedrock exposures near the upper and middle portions of the crater walls. Most occur along the rim crest, but several are located immediately below the contact between the Kaibab and Toroweap (Kumar *et al*., 2010). The widths of the alcoves range from ~10 to ~120 m, the largest of which are associated with the portions of the crater affected by tear faults (*e.g.*, as in the southeast and southwest corners of the crater). These alcoves would have formed from precipitation falling directly on the rim of the crater.

A few small alcoves exist at the base of a fracture system through the Kaibab appear to have been carved by precipitation that flowed down through that fracture system where it was then discharged through the underlying Toroweap sandstone. The pathways through the Kaibab are so efficient at dewatering the unit that there are no perennial streams on the Kaibab plateaus surrounding the Grand Canyon (Huntoon, 2000).

In general, the alcove-channel erosional process removed material from the rim and upper wall of the crater, transported it downward along channels <1 to ~5 m wide, and deposited it along the base of the crater wall or on the crater floor (Kumar *et al.*, 2010). The channels produced by that flow cut through a veneer of colluvium on the crater wall, reworking that material a second time. Incision was also greatest in the weakest lithologies on the crater wall: *e.g.*, in authigenic fault breccias and impact breccias.

Some of that sediment transport occurred (and still occurs) in an ephemeral alluvial process that produced meandering channels and outwash deposits on the lowest slopes and crater floor. However, the lower walls of the crater are also cross-cut by dramatic m-scale boulder-levee channels indicative of debris flows (Fig. 15.8 through 15.10). That type of rock flow and levee construction is common in arid environments following short bursts of precipitation that mix relatively small amounts of water (*c.* 20%) with unconsolidated debris (*c.* 80%). While those debris flow channels were briefly described by Kumar *et al.* (2010), they were the focus of the mass wasting study of Palucis *et al.* (2012a,b; 2015).

LiDAR maps (Fig. 4.3) were used to map the distribution of those debris flow channels around the crater. Field studies of representative channels were then made to assess the type of debris involved, its size distribution, the contrast in size distributions between the channel fill and levees, and the point in the channel where the transition from entrainment to deposition began. For example, in a debris flow channel in the northeast quadrant of the crater (Fig 15.9), levees were ~4 to 6 m apart and ~0.5 to 0.7 m tall. Some boulders in the levees are more than 0.5 m in diameter (Palucis *et al.*, 2012a). Cosmogenic nuclide analyses of boulders in the levees produced ages of ~10.1 to 18.7 ka, suggesting the debris flow channel was last active during the Pleistocene.

Those field observations then guided a series of rotating drum experiments to determine the amount of water needed to transport the debris. Assuming a water-to-rock ratio of 0.3 in the debris flows, Palucis *et al.* (2015) estimated ~150,000 m^3 of water transported ~500,000 m^3 of debris. The erosional events required <0.4 m of total runoff over the 0.35 km^2 upslope source area of the crater, which corresponds to ~26 mm of runoff per debris flow event. Based on the measured cosmogenic nuclide ages of a boulder

levee, the debris flow activity apparently ceased in the early Holocene when the crater lake disappeared and the surrounding region became more arid.

Those two studies were tremendously illuminating, but several questions still remain. Which type of process, fluvial of debris flow, dominated erosion? Did the debris flows reach the edge of the lake and, if so, what happened? Can the lengths of debris flows or the morphologies of their distal ends be used to determine the size of the lake over time? Did the lake shrink monotonically or did it oscillate in size? Additional studies of the gully system and its channels, like studies of the lake sediments (Chapter 14), should provide a better assessment of the post-impact modification of the crater and the evolution of the Colorado Plateau climate during the past ~50,000 years.

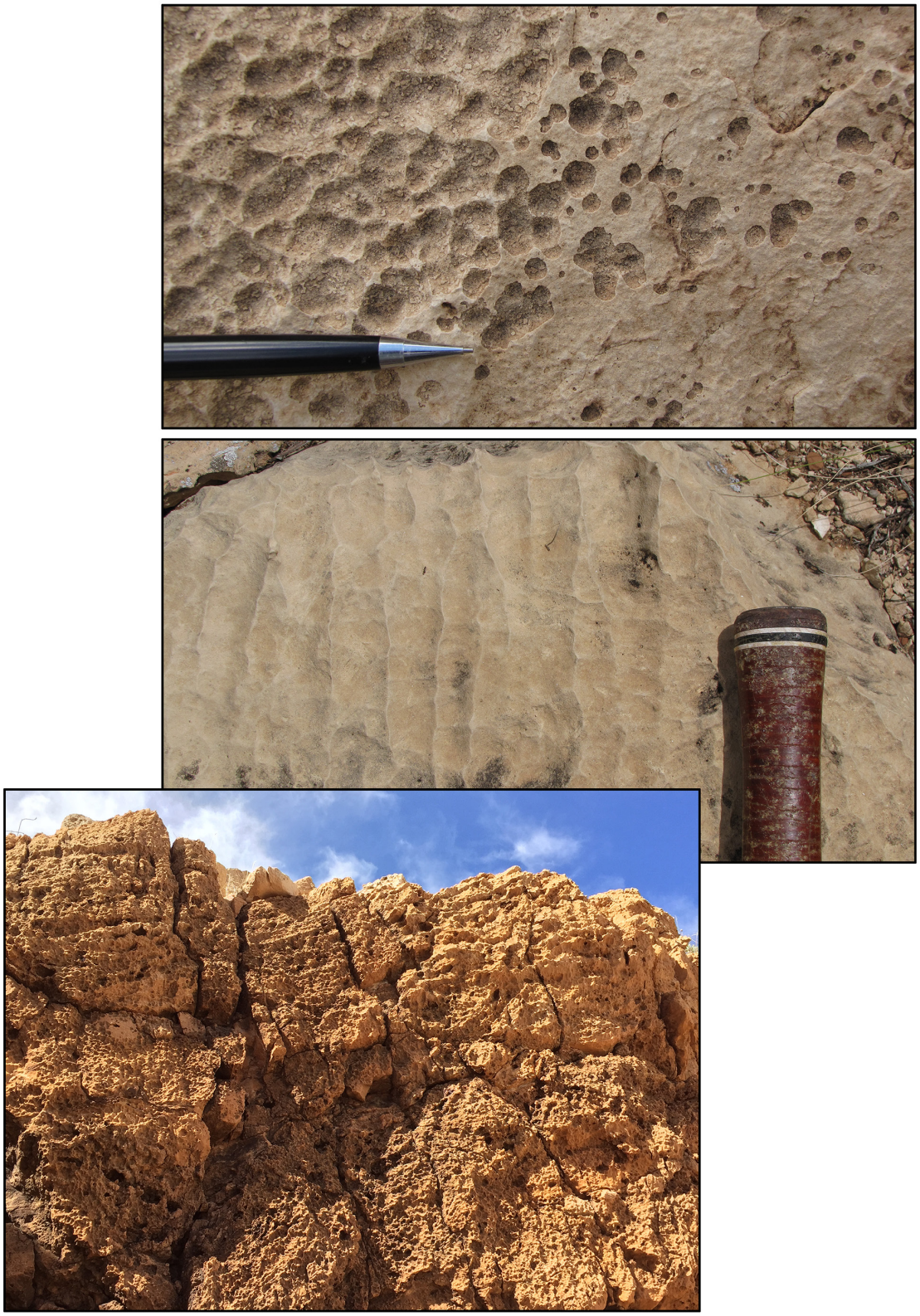

Fig. 15.1. Differential dissolution and flaking on surface of ejected Kaibab boulder (top panel), where incipient solution pits in case-hardened surface (right) occurs adjacent to well-developed solution pits (left). Near-vertical alignment of solution pits reflecting water flow downward along the face of an ejected Kaibab boulder (middle panel). Extreme example of dissolution in bedrock Kaibab in crater wall, along trail to the crater floor in the northwest portion of the crater.

Fig. 15.2. Differential erosion (top panel) where the top of the rock has been exposed to weathering far longer than the lower portion of rock, which was likely buried. The top of the rock has lost a significant layer of material (where hammer sits) and also has much deeper solution pits. Dissolution of an ejected Kaibab boulder (bottom two panels) has completely separated small breakdown blocks, as illustrated in the bottom image where the loose segments have been manually overturned.

Fig. 15.3. Tafoni at three different scales in the Wupatki Mbr of the Moenkopi Formation. Centimeter-scale pits occur on the surface of an ejected boulder (top). Decimeter-scale pits occur in bedrock on the south crater wall (middle panel). Meter-scale cavernous openings also occur around the crater, as seen here on the south crater wall. The interior of the cavern is being utilized by fauna. See Kring and Andes (2016).

Fig. 15.4. Pre-impact features on target Moenkopi can affect its post-impact breakdown in the ejecta blanket. Tafoni will sometimes form along laminae in the cross-bedded siltstone (top). Also, joints and bedding planes are weaknesses that accelerate breakdown (bottom). A student, Ankit Verma, and his advisor, Mary Bourke, are currently studying the breakdown of Moenkopi and Coconino. A 33-cm-long hammer for scale.

Fig. 15.5. Caliche coatings on (from top to bottom) Moenkopi siltstone, Kaibab sandy carbonate, Coconino sandstone, all from Barringer Crater, and a porphyritic olivine basalt from the San Francisco Volcanic Field near Flagstaff. Samples MC71108-4a, MC71108-1b, MC71108-3, and SFVF71008-2a. A 1-cm cube is included for scale.

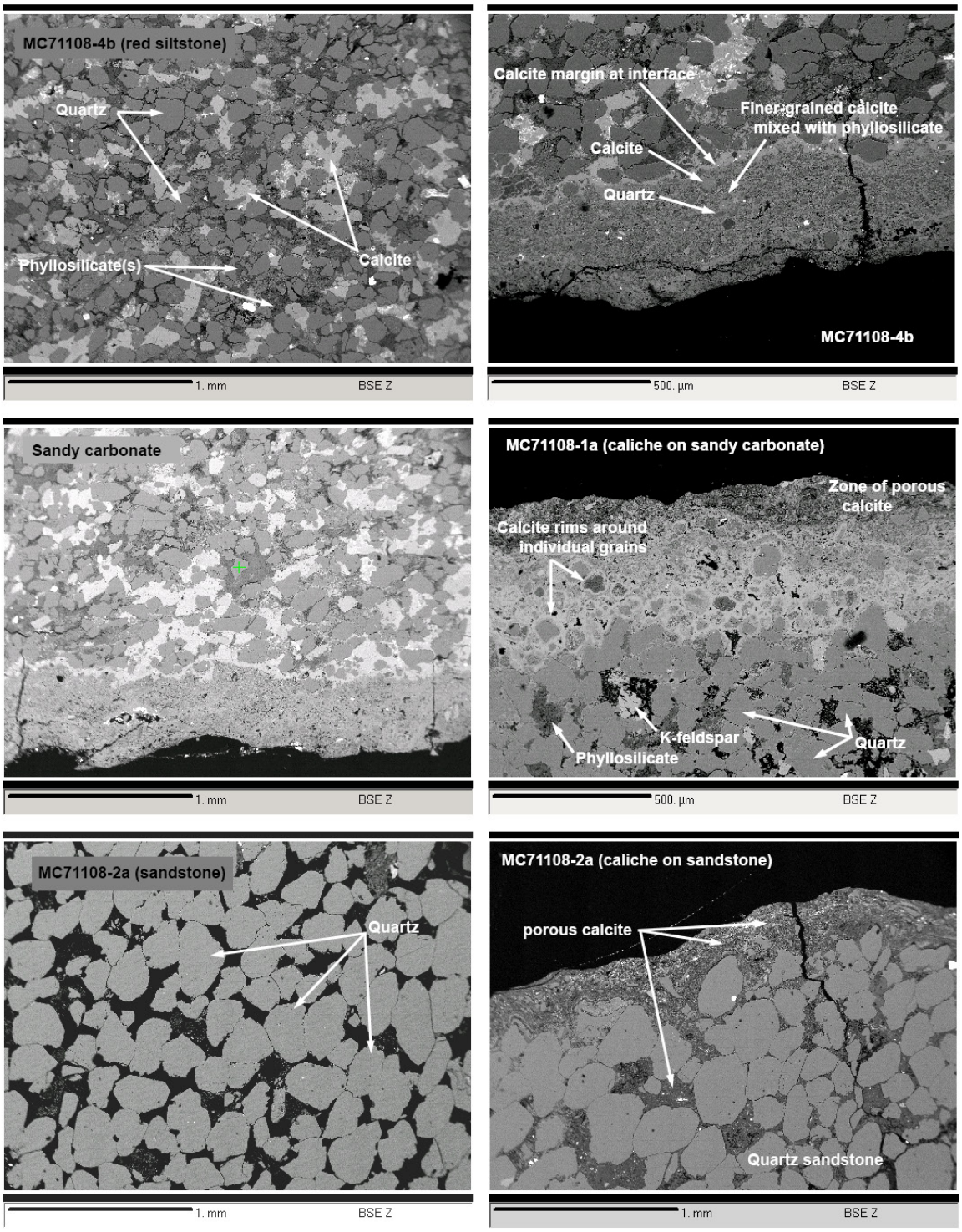

Fig. 15.6. Ejected sample of Moenkopi red siltstone (top left) with a caliche coating (top right). Ejected sample of Kaibab sandy carbonate with caliche coating (second row). Multiple layers indicate changing diagenetic (likely climate-related) conditions (second row right). Ejected sample of Coconino sandstone (third row left) with a caliche coating (third row right). Phyllosilicates (clay) can also be comingled, in variable proportions, with the carbonate in the caliche coatings. Backscattered electron images. Samples MC71108-4b, MC71108-1a, and MC71108-2a. Scale bars are either 1 mm or 0.5 mm (500 µm).

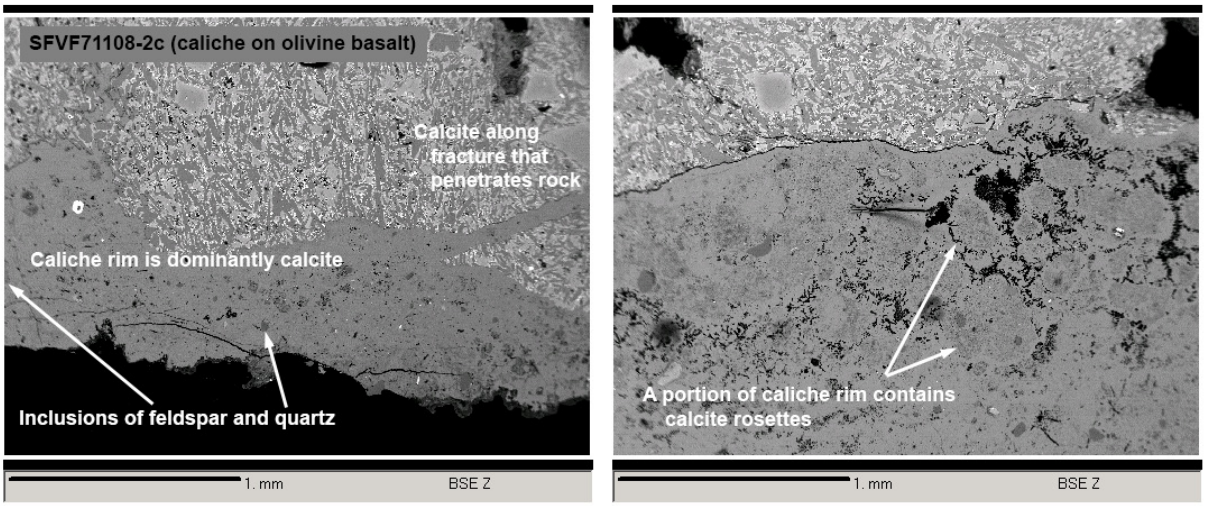

Fig. 15.7. For comparison with the Barringer Crater samples shown in Fig. 15.6, here are shown caliche coatings on a porphyritic olivine basalt from the nearby San Francisco Volcanic Field. When the calcium carbonate precipitated around the basalt, it also entrained and cemented other phases in the soil; *e.g.*, feldspar and quartz (bottom left panel). Phyllosilicates (clay) can also be comingled, in variable proportions, with the carbonate in the caliche coatings. Backscattered electron images. Sample SFVF71008-2c. Scale bars are 1 mm.

Fig. 15.8. Leveed debris flow channels can be seen from the crater rim. An example appears here in the center of the field of view. Several older leveed channels are also visible. Sometimes a channel will cut across an older channel. East side of the crater.

Fig. 15.9. Below gully alcoves, gullies often transition to debris flow channels with boulder levees. The lower left panel is a view looking down a channel on the east crater wall that flows out onto the crater floor. The upper right panel is a close-up view of a boulder-rich levee along one of these types of channels. A person is in the field of view in the lower left panel for scale. A 33-cm-long hammer is shown for scale in the upper right panel.

Fig. 15.10. In this perspective view, a debris flow channel with a boulder-rich levee is in the foreground and rises in the distance towards its source region on the south crater wall. Yellow arrows point to the margin of the gully as it rises up the crater wall.